Reactions of Laser-Ablated Niobium, Tantalum, and Rhenium Atoms with Nitrogen Atoms and Molecules. Infrared Spectra and Density Functional Calculations of the Metal Nitride and Dinitride Molecules

Mingfei Zhou and Lester Andrews*

Department of Chemistry, University of Virginia, Charlottesville, Virginia 22901

Received: June 30, 1998; In Final Form: September 1, 1998

Laser-ablated niobium, tantalum, and rhenium atoms have been reacted with nitrogen atoms and molecules during condensation in excess argon and in pure nitrogen gas. Metal nitride molecules NbN, TaN, ReN, and their dinitrogen complexes were trapped and identified by nitrogen isotopic shifts and DFT frequency calculations. The NbN_2 and TaN_2 dinitride molecules were produced on annealing in solid nitrogen and on deposition and increased on photolysis in solid argon. Metal dinitrogen complexes were also observed for each metal.

Introduction

Niobium, tantalum, and rhenium nitrides are of interest owing to their application for coatings, superconductors, and synthesis.[1,2] However, most of the previous investigations have been devoted to nitride film fabrication and characterization, and little is known about the gas-phase reactions of the metal atoms with nitrogen. Electronic spectra of niobium nitride molecules have been studied in the gas phase and in solid argon, the dipole moment has been measured, and the ground electronic state identified as a $^3\Delta$ configuration.[3−5] Niobium is of special interest owing to its large ($I = {}^9/_2$) nuclear spin. The vibrational fundamentals of NbN and TaN have been determined by infrared absorption spectra in the argon matrix using a sputtering source.[3,6] Recently, rhenium nitride has been synthesized in the gas phase using laser ablation, and high-resolution electronic emission spectra have been observed.[7]

Pulsed-laser ablation of a metal target produces highly reactive metal species such as metastable excited states and high kinetic energy atoms[8] and provides an effective method for the synthesis of molecules that cannot be obtained by thermal metal atom reactions.[9−11] By co-deposition of laser-ablated metal atoms with nitrogen in excess argon and with pure nitrogen, the metal nitrides and dinitrogen complexes of V, Cr, Mn, Fe, Ni, and Co have been trapped in solid argon and nitrogen, and studied using infrared spectroscopy.[9−11] In this paper, we report similar studies on reactions of laser-ablated niobium, tantalum, and rhenium atoms with nitrogen molecules. We will show that in addition to diatomic nitrides, metal dinitrides as well as dinitrogen complexes are observed and identified via isotopic substitution and density functional calculations.

Experimental Section

The experiments of laser ablation and FTIR matrix investigation have been described previously.[9−11] The 1064 nm Nd:YAG laser beam (*Spectra Physics*, DCR-11) was focused by a 10 cm focal length lens onto the rotating metal target. The laser employed a repetition rate of 10 Hz with pulse width of 10 ns; laser energies ranging from 40 to 80 mJ/pulse were used in the experiments. The ablated metal atoms were co-deposited with pure nitrogen as well as 2% N_2 in argon onto the 10 K CsI window at a rate of 2−4 mmol/h for 1−2 h. Isotopic nitrogen $^{15}N_2$ (99.9%) and $^{14}N_2 + {}^{15}N_2$ mixtures (50%/50%) were used. FTIR spectra were recorded with 0.5 cm^{-1} resolution and 0.1 cm^{-1} accuracy on a Nicolet 750 instrument. Matrix samples were annealed at different temperatures, and selected samples were subjected to broadband photolysis by a medium-pressure mercury arc lamp (Phillips, 175W) with the globe removed (240−580 nm).

Results

Infrared spectra and density functional calculations of laser-ablated Nb, Ta, and Re atom reaction products will be presented in turn.

Nb + N_2. Laser-ablated Nb atoms were co-deposited with pure nitrogen, and the product absorptions are listed in Table 1. In the upper wavenumber region, strong bands at 2087.8 and 2071.7 cm^{-1} were observed after deposition. These bands increased slightly on annealing and on photolysis, while another sharp band at 2134 cm^{-1} increased markedly on annealing but decreased on photolysis. Weak bands at 1965.2 and 1815.6 cm^{-1} were observed after deposition, and both decreased on annealing, which produced another weak band at 1857.1 cm^{-1}. In additional, sharp bands at 1657.6 and 2003.0 cm^{-1} due to N_3 and N_3^- were also observed in this region (Figure 1).

Spectra in the lower region revealed a 965.6 cm^{-1} band, which increased on annealing, together with weak bands at 974.3 and 976.8 cm^{-1} (Figure 2). A pair of doublets at 889.6, 888.4 cm^{-1} and 651.0, 649.0 cm^{-1} appeared and grew together on annealing; meanwhile, weak bands at 769.8, 724.9, and 569.6 cm^{-1} were produced on annealing. Strong bands at 523.0, 519.4, and 458.4 cm^{-1} were detected in the low-frequency region (not shown); these bands decreased on annealing while another strong band at 439.2 cm^{-1} increased.

Isotopic experiments were done using $^{15}N_2$ and $^{14}N_2 + {}^{15}N_2$ samples. The spectra with $^{15}N_2$ were similar to those with $^{14}N_2$, and all of the product absorptions shifted as listed in Table 1. In the isotopic mixture experiments, a pentet structure was observed for the 523.0 cm^{-1} band with intermediate components at 519.6, 515.8, and 512.1 cm^{-1}, and triplets were observed for the 889.6, 888.4 cm^{-1} and 651.0, 649.0 cm^{-1} bands with

10.1021/jp982814w CCC: $15.00
Published on Web 10/21/1998

TABLE 1: Infrared Absorptions (cm^{-1}) from Laser-Ablated Niobium Atoms Co-deposited with Pure Nitrogen at 10 K

$^{14}N_2$	$^{15}N_2$	$^{14}N + {}^{15}N_2$	R(14/15)	assignment
2327.5	2249.8	2327.3, 2249.6	1.0345	N_2 perturbed
2323.0	2245.5		1.0345	$(NN)_xNbN_2$
2320.4	2243.0		1.0345	$(NN)_xNbN_2$ site
2224.0	2149.8		1.0345	$(NN)_xNbN$
2222.3	2148.6		1.0343	$(NN)_xNbN$
2140.2	2069.1		1.0344	$Nb(NN)_6$ site
2134.8	2063.8	doublet	1.0344	$Nb(NN)_6$
2128.8	2058.3		1.0343	$Nb(NN)_x$
2121.3	2051.0		1.0343	$Nb(NN)_x$
2097.5	2028.3		1.0342	$Nb(NN)_x$
2094.4	2024.6		1.0345	$Nb(NN)_x$
2087.8	2018.4		1.0344	$Nb(NN)_x$
2071.7	2003.1	doublet	1.0343	$Nb(NN)_4$
2061.6	1993.3		1.0343	$Nb(NN)_4$ site
2003.0	1937.2		1.0340	N_3^-
1974.5	1908.7		1.0345	NbNN site
1965.2	1899.9	doublet	1.0344	NbNN
1857.1	1795.4	doublet	1.0344	$(NN)_xNb(N_2)$
1815.6	1755.6	doublet	1.0342	$Nb(N_2)$
1657.6	1603.2	1657.7, 1649.3, 1612.9, 1603.2	1.0339	N_3
976.8	948.2	doublet	1.0302	$(NN)_xNbN$
974.3	945.7	doublet	1.0302	$(NN)_xNbN$
972.2	943.6	doublet	1.0303	$(NN)_xNbN$
969.2	940.9	doublet	1.0301	$(NN)_xNbN$
968.6	940.2	doublet	1.0302	$(NN)_xNbN$
965.6	937.3	doublet	1.0302	$(NN)_xNbN$
889.6	863.0	889.5, 876.9, 863.1	1.0307	$(NN)_xNbN_2$
888.4	861.8	888.3, 875.6, 862.0	1.0309	$(NN)_xNbN_2$
769.8	748.0		1.0291	? Nb_2N
724.9	703.0		1.0312	? Nb_2N_2
651.0	632.1	651.0, 641.1, 632.3	1.0299	$(NN)NbN_2$
649.0	630.4	648.9, 639.2, 630.4	1.0295	$(NN)NbN_2$
569.6	552.1		1.0317	? Nb_2N_2
523.0	507.4	523.0, 519.6, 515.8, 512.1, 504.0	1.0306	$Nb(NN)_4$
519.2	504.0		1.0302	$Nb(NN)_4$ site
475.1	462.5		1.0272	$Nb(NN)_x$
458.6	445.3	458.2, 452.1, 445.1	1.0299	$Nb(NN)_x$
439.4	426.6		1.0300	$Nb(NN)_6$
436.0	423.7		1.029	$Nb(NN)_6$ site

intermediates at 876.9, 875.6 cm^{-1} and 641.1, 639.2 cm^{-1}. Only pure isotopic counterparts were observed for the bands with "doublet" given in Table 1.

Nb + N_2/Ar. Infrared spectra of laser-ablated niobium atoms co-deposited with 2% N_2 in argon are shown in Figures 1 and 2 for selected regions, and the absorption bands are listed in Table 2. In the low-wavenumber region, weak bands at 1001.3, 993.5, and 986.5 cm^{-1} increased slightly on 25 K annealing and decreased on higher temperature annealing, which produced a new absorption at 974.2 cm^{-1}. Two doublets at 914.9, 918.6 and 680.8, 685.4 cm^{-1} were observed on deposition; these bands increased on first annealing and on broadband photolysis, and then decreased on subsequent annealing to 40 K. Below 500 cm^{-1}, weak bands at 470.9 and 439.8 cm^{-1} were produced on annealing. In addition, weak bands at 970.6 and 875.8 cm^{-1} due to niobium oxides[12] were observed after deposition.

Spectra in the 2300−1600 cm^{-1} region were complicated. Broad bands peaked at 1924.8 and 1987.9 cm^{-1} were observed after deposition. After annealing to 25 K, the former band decreased and the later band increased. Subsequent annealing to 30, 35, and 40 K evolved the bands to higher frequency with major bands at 2136.2 and 2072.5 cm^{-1}.

Similar spectra were obtained using the $^{15}N_2$/Ar sample. The 1001.3, 993.5, and 986.5 cm^{-1} bands shifted to 972.2, 964.6, and 957.7 cm^{-1}, respectively. The doublet at 914.9, 918.6 cm^{-1} shifted to 891.5, 887.8 cm^{-1}, while the 685.4, 680.8 cm^{-1} doublet shifted to 665.9, 661.3 cm^{-1}. All absorptions in the upper region yielded isotopic shifts. The mixed $^{14}N_2$ + $^{15}N_2$ sample gave weak intermediate bands at 905.6 and 671.5 cm^{-1}; however, in the upper region the spectrum was congested, which made the identification of intermediate bands impossible.

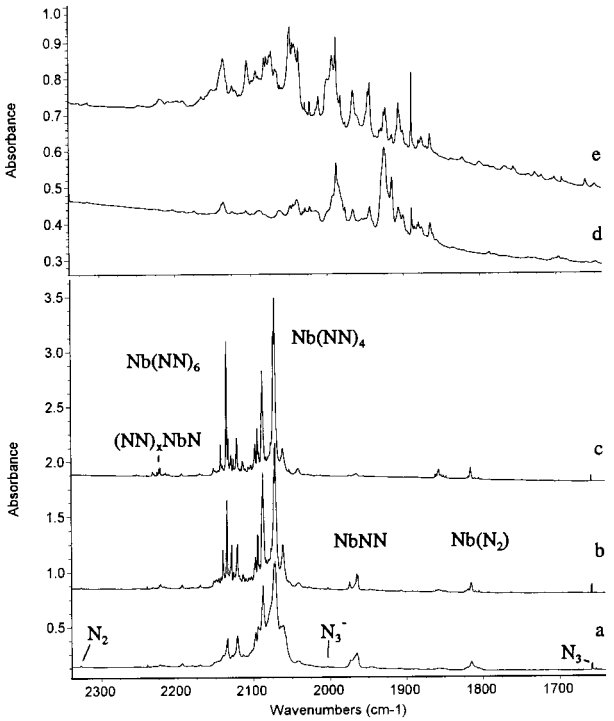

Figure 1. Infrared spectra in the upper region for laser-ablated Nb atoms co-deposited with nitrogen at 10 K: (a) Nb atoms in pure dinitrogen, (b) after annealing to 25 K, (c) after annealing to 35 K, (d) Nb atoms in argon with 2% N_2, and (e) after 35 K annealing.

Ta + N_2. Similar spectra were obtained for laser-ablated Ta co-deposited with N_2, as shown in Figures 3 and 4. Strong bands were observed at 2040.9, 2102.8 cm^{-1} and 457.8, 453.5 cm^{-1} after deposition, while annealing decreased the 2040.9, 457.8 cm^{-1} bands and increased the 2102.8, 453.5 cm^{-1} bands. Additional weak bands were also observed at 1947.6, 1810.7, and 1762.6 cm^{-1} after deposition. In the middle region, a 962.8 cm^{-1} band observed after deposition increased together with weak bands around 968.3 and 970.9 cm^{-1}. Also sharp bands were produced at 895.2, 822.1, 770.2, 760.9, 731.0, and 693.3 cm^{-1} during annealing. The $^{15}N_2$ sample gave shifted bands as listed in Table 3.

Mixed isotopic experiments were done for band identification. The bands between 979.5 and 961.9 cm^{-1} and bands at 1947.6, 1810.7, and 1762.6 cm^{-1} showed pure isotopic bands with no intermediate components. However, the 2040.9 cm^{-1} band showed three weak intermediate bands at 2007.8, 1997.7, and 1989.2 cm^{-1}, and associated peaks at 2149.6, 2139.7, and 2128.4 cm^{-1}. The 895.2 and 693.3 cm^{-1} bands showed new intermediate bands at 882.0 and 681.9 cm^{-1}, and a triplet of doublets was observed for the 770.2 cm^{-1} band.

Ta + N_2/Ar. Laser-ablated Ta atoms were co-deposited with 2% N_2 in argon. A new absorption centered at 1058.8 cm^{-1} with site bands at 1063.0, 1057.3, and 1055.7 cm^{-1} was observed after deposition; on annealing, the site bands decreased and only the 1058.8 cm^{-1} band remained after 40 K annealing. In the $^{15}N_2$ experiment, these bands shifted to 1029.8, 1025.9, 1024.5, and 1022.8 cm^{-1}. Weak bands at 924.2, 922.7, 814.8, 813.1, 799.7, 770.7, 751.2, and 740.3 cm^{-1} were observed after deposition and decreased on annealing. All of the bands

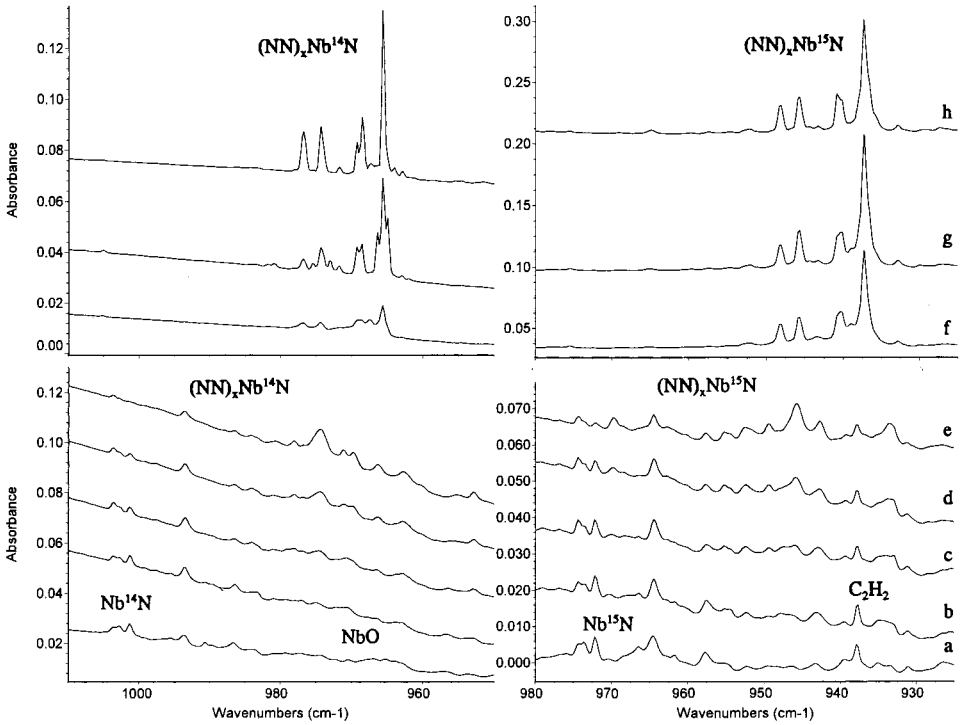

Figure 2. Infrared spectra in the lower region for laser-ablated Nb atoms co-deposited with $^{14}N_2$ (left) and $^{15}N_2$ (right): (a) Nb atoms in argon with 2% N_2, (b) after annealing to 25 K, (c) after annealing to 30 K, (d) after annealing to 35 K, (e) after annealing to 40 K, (f) Nb atoms with pure dinitrogen, (g) after annealing to 25 K, and (h) after annealing to 35 K.

TABLE 2: Infrared Absorptions (cm^{-1}) from Laser-Ablated Niobium Atoms Co-deposited with 2% N_2 in Argon

$^{14}N_2$	$^{15}N_2$	*R*(14/15)	assignment
2136.2	2065.1	1.0344	$Nb(NN)_6$
2105.2	2034.9	1.0346	$Nb(NN)_x$
2072.5	2003.7	1.0343	$Nb(NN)_4$
2049.7	1981.4	1.0345	$Nb(NN)_x$
1987.9	1922.1	1.0342	$Nb(NN)_x$
1965.6	1900.5	1.0343	$Nb(NN)_x$
1943.7	1879.2	1.0343	$Nb(NN)_x$
1914.5	1851.2	1.0342	NbNN
1905.6	1842.4	1.0343	NbNN site
1888.7	1826.0	1.0343	$Nb(N_2)$
1864.2	1802.9	1.0343	$Nb(N_2)$ site
1001.3	972.2	1.0299	NbN
993.5	964.6	1.0300	$(NN)_xNbN$
986.5	957.7	1.0301	$(NN)_xNbN$
974.2	945.9	1.0299	$(NN)_xNbN$
970.6	940.6		NbO
962.5	933.7	1.0309	$(NN)_xNbN$
918.6	891.5	1.0304	NbN_2
914.9	887.8	1.0305	NbN_2
875.8	875.8		NbO_2
861.3	861.3		$(N_2)NbO_2$
685.4	665.9	1.0293	NbN_2
680.8	661.3	1.0295	NbN_2
470.9	457.4	1.0295	$Nb(NN)_x$
439.8	427.2	1.0295	$Nb(NN)_6$

exhibited isotopic shifts using $^{15}N_2$/Ar, and no obvious intermediate bands were observed using 2% $^{14}N_2$ + 2% $^{15}N_2$ in argon.

The spectrum in the 2200−1600 cm^{-1} region was complicated. Broad bands at 1933.7, 1952.8, 2009.0, 2041.9, and 2106.4 cm^{-1} were observed. After annealing to 40 K, the bands at 2106.4 and 2063.0 cm^{-1} dominated the spectra.

Re + N_2. The co-deposition of Re atoms with pure N_2 gave strong bands at 2100.6, 2097.7, 2087.8, 2083.5, 2073.4, and 2071.5 cm^{-1}. Annealing sharpened and decreased the 2100.6, 2097.7, and 2087.8 cm^{-1} bands and increased the 2083.5 and 2071.5 cm^{-1} bands, which dominated the spectra after higher temperature annealing. Weak bands at 1984.5, 1982.2, 1944.7, 1941.9, 1894.7, and 1885.8 cm^{-1} observed after deposition decreased on annealing. Otherwise, sharp bands at 2226.9, 2204.6 cm^{-1} and 1744.1, 1742.3, 1740.2 cm^{-1} appeared on annealing in the upper region (Figure 5).

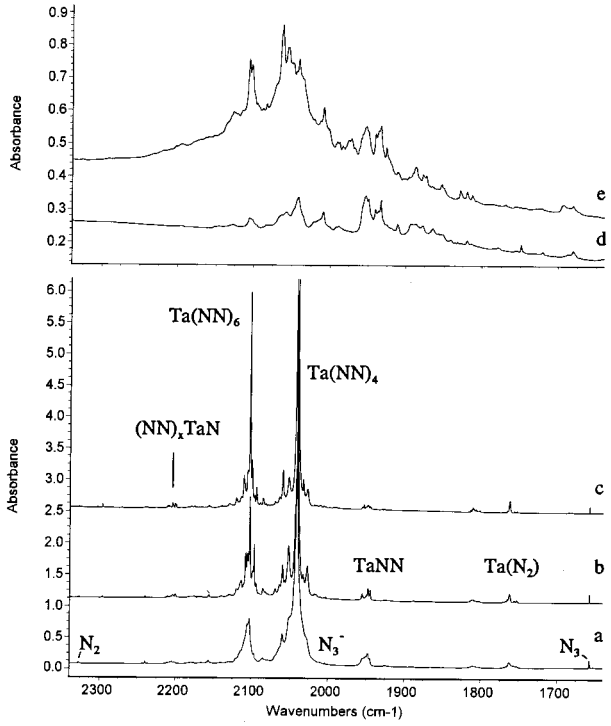

Figure 3. Infrared spectra in the upper region for laser-ablated Ta atoms co-deposited with nitrogen at 10 K: (a) Ta atoms in pure dinitrogen, (b) after annealing to 25 K, (c) after annealing to 35 K, (d) Nb atoms in argon with 2% N_2, and (e) after 35 K annealing.

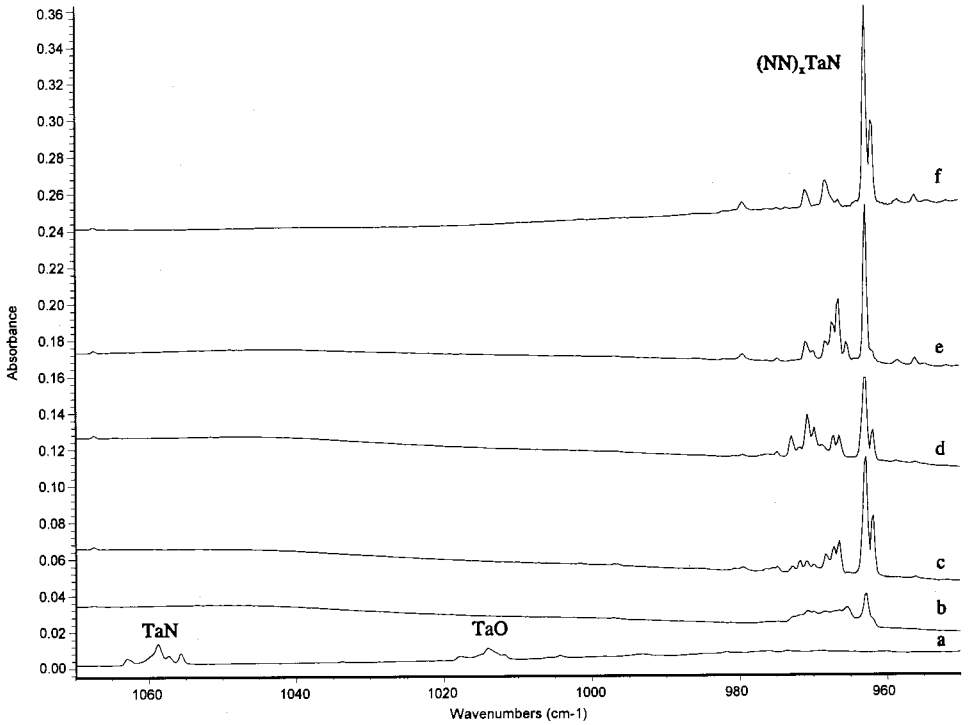

Figure 4. Infrared spectra in the lower region for laser-ablated Ta atoms co-deposited with nitrogen at 10 K: (a) Ta atoms in argon with 2% N_2, (b) Ta atoms with pure dinitrogen, (c) after annealing to 25 K, (d) after broadband photolysis, (e) after annealing to 30 K, and (f) after annealing to 35 K.

In the middle region, a strong doublet was observed at 1084.8, 1083.6 cm^{-1} after deposition; annealing decreased the 1084.8 cm^{-1} band and increased the 1083.6 cm^{-1} band, while photolysis reversed the two peaks. Weak sharp bands at 1116.1, 1089.3, and 1086.7 cm^{-1} also appeared on 25 K annealing and then decreased (Figure 6). After 30 K annealing, the 1084.8 cm^{-1} band disappeared leaving the 1083.6 cm^{-1} band. Meanwhile, a sharp band appeared at 816.5 cm^{-1} on 25 K annealing, decreased on photolysis, and markedly increased on 30 K annealing. In the low region, broad bands at 522.6, 511.4 cm^{-1} observed after deposition decreased on annealing, while two sharp bands at 439.7 and 436.2 cm^{-1} greatly increased.

Again, isotopic $^{15}N_2$ and $^{14}N_2 + {}^{15}N_2$ mixture were employed. All the bands exhibited $^{15}N_2$ shifts, as listed in Table 4, and the mixture gave doublets for bands between 1083.6 and 1116.1 cm^{-1} and a 1/2/1 triplet at 816.5, 803.6, 792.8 cm^{-1}. Figure 7 shows the 0.125 cm^{-1} resolution spectrum (recorded specifically to resolve Re isotopes) for the two strong peaks after 30 K annealing to give a single matrix site. The resolved 1:2 relative intensity rhenium isotopic bands were 1083.84, 1083.45 cm^{-1} and 1050.01, 1049.62 $\pm$ 0.02 cm^{-1} for ^{14}N and ^{15}N, respectively, with peak full widths at half-maximum of 0.17 $\pm$ 0.02 cm^{-1}.

Re + N_2/Ar. Laser-ablated Re atoms co-deposited with N_2 in excess argon gave a weak peak at 1121.4 cm^{-1} and a doublet at 1117.2 and 1115.8 cm^{-1}, which slightly increased and then decreased on annealing, while two bands appeared at 1084.5 and 1079.1 cm^{-1}. In the $^{15}N_2$ experiment, these bands shifted to 1086.2, 1082.3, 1080.9, 1050.5 and 1045.6 cm^{-1}, respectively, and no intermediate bands were observed using mixed isotopic sample (Figure 6 and Table 6). In the upper region, weak bands at 1966.2 and 1940.1 cm^{-1} increased on 25 K annealing, and another annealing to 30 K increased these bands and produced two new bands at 2058.4 and 2033.4 cm^{-1}. Photolysis markedly decreased the three higher frequency bands and produced bands at 2131.0, 2084.0, and 2050.0 cm^{-1}. All of these bands shifted with $^{15}N_2$ (Table 6). A doublet for the 1940.1 cm^{-1} band and a triplet for the 1966.2 cm^{-1} band with intermediate at 1919.0 cm^{-1} were observed using the mixed isotopic sample. For the bands above 2000 cm^{-1}, the identification of intermediate components was not possible owing to congestion.

Calculations. Density functional theory calculations using the Gaussian 94 program[13] were employed to calculate structures and frequencies for the simplest products expected here in order to provide a guide for the experimental identification of new molecules. The BP86 functional, D95* basis set for nitrogen and Los Alamos ECP plus DZ basic set for metal atoms were used for all calculations.[14−16] Calculations were done for NbN and TaN in singlet and triplet and ReN in triplet and quintet states, and the results are listed in Table 7. Our DFT investigations are in excellent agreement with (FO + MRSD) CI calculations of bond length (1.695 Å) and harmonic frequency (1010 cm^{-1}) for the $^3\Delta$ ground state of NbN.[6] The triplet was calculated lower in energy for both NbN and ReN, while the singlet state was lower for the TaN molecule. We are not aware of previous calculations for tantalum and rhenium nitrides. The bent NN−NbN, NN−TaN, and NN−ReN "complex" molecules were also calculated; all three molecules exhibited triplet ground states as listed in Table 5 and red-shifted M−N stretching modes. It is interesting to note that, for the NNTaN complex, the triplet state was lower in energy, while the singlet was the lower state for TaN. Hence, NN complexing reversed the energy ordering of the electronic states of the TaN molecule.

Similar calculations were also performed on three MNN isomers, and the results are listed in Table 8. The linear sextet NbNN molecule was the most stable isomer followed by bent NNbN and cyclic Nb(N_2) in doublet states, which were only 3.4 and 5.6 kcal/mol higher. For Ta, the most stable isomer was doublet Ta(N_2); doublet NTaN and sextet TaNN were 8.2 and 10.2 kcal/mol higher. Bent NReN was found to be the lowest isomer for this stoichiometry.

TABLE 3: Infrared Absorptions (cm^{-1}) from Laser-Ablated Tantalum Atoms Co-deposited with Pure Nitrogen at 10 K

$^{14}N_2$	$^{15}N_2$	$^{14}N_2 + {}^{15}N_2$	R(14/15)	assignment
2327.5	2249.8	2327.3, 2249.6	1.0345	N_2 perturbed
2296.9	2200.3		1.0345	$(NN)_xNTaN_2$
2204.6	2131.1		1.0345	$(NN)_xTaN$
2201.4	2128.1		1.0344	$(NN)_xTaN$
2108.3	2038.3		1.0343	$Ta(NN)_6$ site
2102.8	2033.0		1.0343	$Ta(NN)_6$
2097.0	2029.0		1.0335	$Ta(NN)_x$
2059.8	1991.5		1.0343	$Ta(NN)_x$
2052.2	1984.0		1.0344	$Ta(NN)_x$
2040.9	1973.4	2149.6, 2139.7, 2128.4, 2040.9, 2007.8, 1997.7, 1989.2, 1937.4	1.0342	$Ta(NN)_4$
2027.6	1961.0		1.0340	$Ta(NN)_4$ site
2003.0	1937.2		1.0340	N_3^-
1955.3	1890.3		1.0344	TaNN
1947.6	1882.9	1948.0, 1882.8	1.0344	TaNN
1944.9	1880.2		1.0344	TaNN
1810.7	1750.5	1810.3, 1752.4	1.0344	$(NN)_xTa(N_2)$
1762.6	1704.1	1762.3, 1704.3	1.0343	$Ta(N_2)$
1657.6	1603.3	1657.6, 1649.3, 1612.9, 1603.2	1.0339	N_3
979.5	948.8	979.5, 948.8	1.0324	$(NN)_xTaN$
972.8	942.4	972.8, 942.4	1.0323	$(NN)_xTaN$
971.8	941.4	971.8, 941.4	1.0323	$(NN)_xTaN$
970.9	940.5	970.9, 940.5	1.0323	$(NN)_xTaN$
968.3	938.0	968.3, 938.0	1.0323	$(NN)_xTaN$
967.2	937.0	967.2, 937.0	1.0322	$(NN)_xTaN$
966.5	936.3	966.5, 936.3	1.0323	$(NN)_xTaN$
962.9	932.8	962.9, 932.8	1.0323	$(NN)_xTaN$
961.9	931.8	961.9, 931.8	1.0323	$(NN)_xTaN$
895.2	866.9	895.2, 882.0, 866.9	1.0327	$(NN)_xTaN_2$
822.1	796.5	822.1, 803.9, 796.5	1.0321	? Ta_2N_2
770.2	745.5	770.2, 767.5, 760.8, 758.2, 755.6, 768.2, 745.6	1.0331	? $Ta(N_2)_2$
693.3	671.8	693.2, 682.0, 671.8	1.0320	$(NN)_xTaN_2$
671.2	650.3		1.0321	Ta_2N_2
510.2	494.9		1.0309	? TaNN
472.1	456.9		1.0333	$Ta(NN)_x$
463.2	448.8		1.0321	$Ta(NN)_x$
457.8	443.3		1.0327	$Ta(NN)_6$
453.5	440.0		1.0307	$Ta(NN)_4$
447.3	433.9		1.0309	$Ta(NN)_4$ site

Discussion

The co-deposition of laser-ablated metal atoms into pure nitrogen produces N_3 radical absorption at 1657.7 cm^{-1} and the weak N_3^- band at 2003.0 cm^{-1}, which show that N atoms are formed in these experiments.[17,18] Furthermore, the green glow observed on annealing attests to the diffusion and reaction of N atoms.[19]

$$M(\text{excess energy}) + N_2 \rightarrow M + N + N \quad (1)$$

$$M + N \xrightarrow{\text{nitrogen}} (NN)_xMN \quad (2)$$

$$M + N \xrightarrow{\text{argon}} MN(\text{argon}) \quad (3)$$

Nitrides. *NbN.* The weak band at 1001.3 cm^{-1} in the argon matrix decreased on stepwise annealing, while bands at 993.5 and 986.5 cm^{-1} increased on initial annealing to 25 K and then decreased on further annealing, and the 974.2 cm^{-1} band increased. The nitrogen-15 counterparts for these bands at 972.2, 964.6, 957.5, and 945.9 cm^{-1} gave the nitrogen 14/15 isotopic ratios of 1.0299, 1.0300, 1.0301, and 1.0299, respectively. These values are in good agreement with the harmonic diatomic NbN oscillator ratio (1.0302). All of these bands showed no intermediate bands when mixed $^{14}N_2 + {}^{15}N_2$ was used. In solid nitrogen experiments, bands at 965.6, 974.3, and 976.8 cm^{-1} increased on annealing and exhibited the 14/15 ratio of 1.0302. These bands are very close to the dominant 974.2 cm^{-1} band after 40 K annealing in a solid argon matrix. The 1001.3 cm^{-1} band is assigned to the NbN molecule isolated in solid argon, which is in good agreement with the previously reported 1002.5 cm^{-1} value.[3] The increase in intensity of bands at 993.5, 986.5, and 974.2 cm^{-1} in argon and 965.6, 974.3 cm^{-1} in nitrogen during annealing suggests complexation by N_2 in the matrix, so these bands are assigned to $(NN)_xNbN$ complexes. The BP86/DFT calculations for the NbN molecule predicted the triplet state to be 17.4 kcal/mol lower than the singlet state and the harmonic vibrational fundamental at 1034.9 cm^{-1}, which

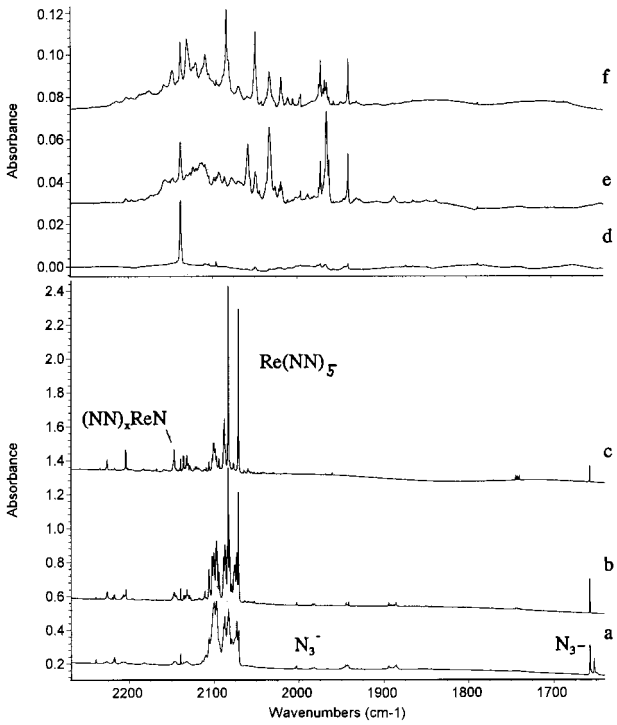

Figure 5. Infrared spectra in the upper region for laser-ablated Re atoms co-deposited with nitrogen at 10 K: (a) Re atoms in pure dinitrogen, (b) after annealing to 25 K, (c) after annealing to 35 K, (d) Nb atoms in argon with 2% N_2, (e) after 30 K annealing, and (f) after broadband photolysis.

TABLE 4: Infrared Absorptions (cm^{-1}) from Laser-Ablated Tantalum Atoms Co-deposited with 2% N_2 in Argon

$^{14}N_2$	$^{15}N_2$	R(14/15)	assignment
2106.4	2036.3	1.0344	$Ta(NN)_6$
2103.1	2033.8	1.0341	site
2063.0	1994.4	1.0344	$Ta(NN)_x$
2056.2	1987.4	1.0346	$Ta(NN)_x$
2041.9	1974.0	1.0344	$Ta(NN)_x$
2009.0	1942.2	1.0344	$Ta(NN)_x$
1952.8	1887.9	1.0344	TaNN
1933.5	1869.2	1.0344	site?
1063.0	1029.8	1.0322	TaN site
1058.8	1025.9	1.0321	TaN
1057.3	1024.5	1.0320	TaN site
1055.7	1022.8	1.0322	TaN site
1014.1	1014.1		TaO
973	942	1.0329	$(NN)_xTaN$
922.7	893.7	1.0324	TaN_2
813.1	787.1	1.0330	?
799.7	774.7	1.0323	?
770.7	746.6	1.0323	?
751.2	728.0	1.0319	?
740.3	717.6	1.0316	TaN_2

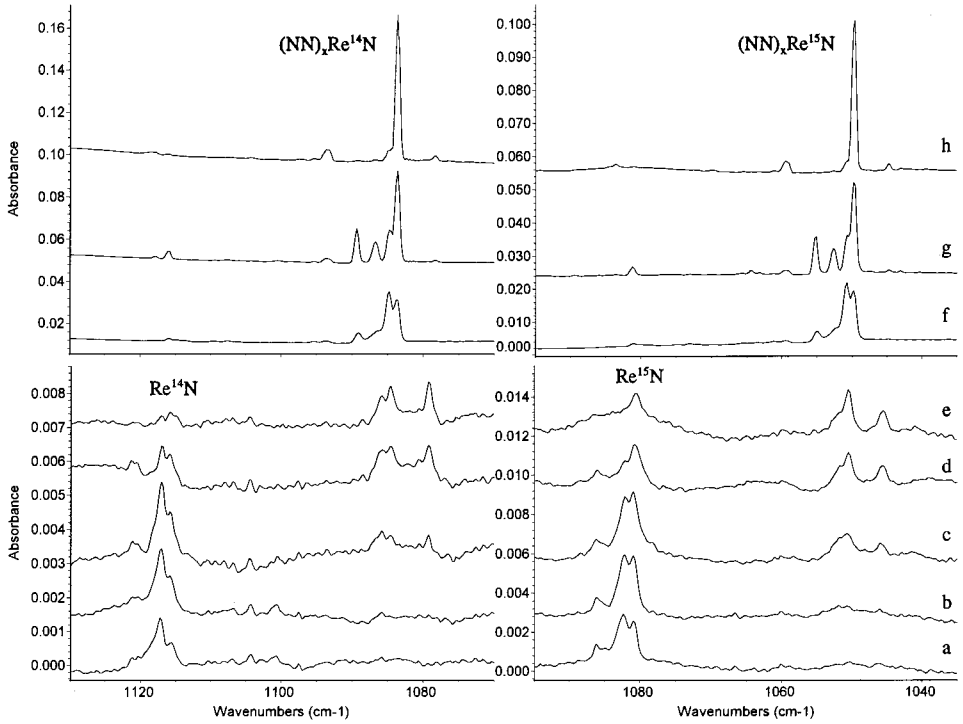

Figure 6. Infrared spectra in the lower region for laser-ablated Re atoms co-deposited with $^{14}N_2$ (left) and $^{15}N_2$ (right): (a) Re atoms in argon with 2% N_2, (b) after annealing to 25 K, (c) after annealing to 30 K, (d) after annealing to 35 K, (e) after annealing to 40 K, (f) Nb atoms with pure dinitrogen, (g) after annealing to 25 K, and (h) after annealing to 35 K.

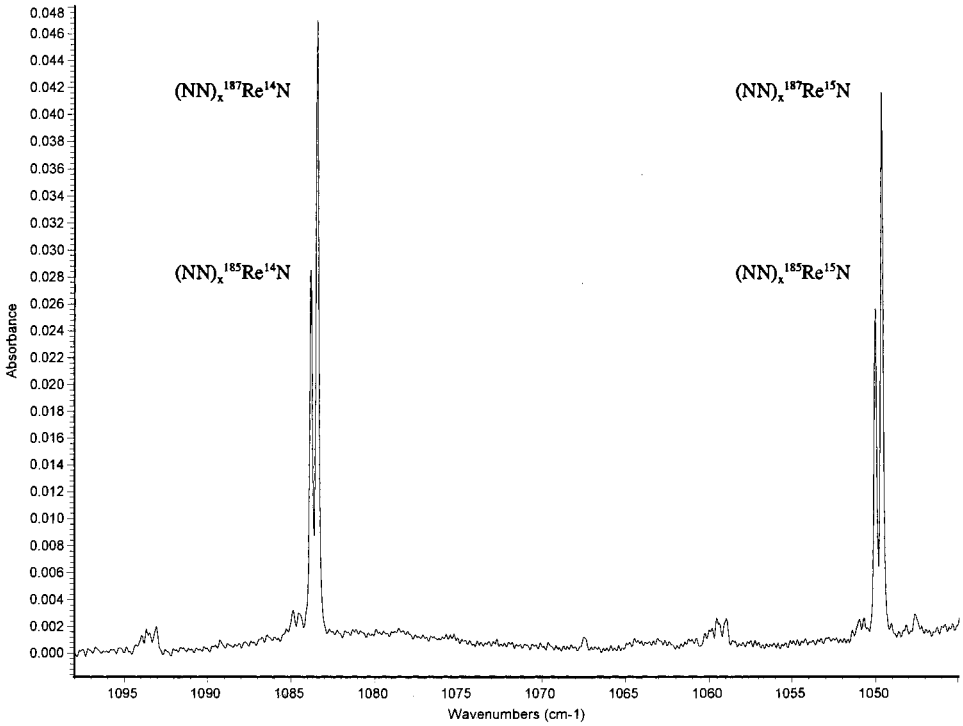

Figure 7. Infrared spectrum recorded at 0.125 cm^{-1} resolution in the low-frequency region for Re atoms co-deposited with pure $^{14}N_2 + {}^{15}N_2$ mixed isotopic sample after annealing to 30 K and recooling to 10 K.

is in good agreement with our experimental frequency (scale factor 0.97). The calculation also showed that N_2 complexation caused the Nb−N stretching vibration to red-shift 5.5 cm^{-1}, very close to the interval between the 1001.3 and 993.5 cm^{-1} bands in the argon matrix.

Pazyuk et al.[5b] reported vibrational constants, which gave a 1035.5 cm^{-1} gas-phase fundamental for NbN, and Azuma et al.[5d] deduced a 1033.8 cm^{-1} vibrational fundamental, noted that this is some 3.1% higher than the matrix value, and suggested that NbN is "fairly highly ionic." However, the dipole moment measured for NbN (3.36 D)[4] is not especially large, and comparable to that for MoN (3.38 D),[4] while the argon matrix fundamental is within 8 cm^{-1} of the gas-phase value.[21,22] Since the NbO molecule is red-shifted 11 cm^{-1} by the solid argon matrix,[12] we suggest that the above deduced gas-phase NbN vibrational frequencies may be too high by $2\omega_e x_e$ or $4\omega_e x_e$ and

TABLE 5: Infrared Absorptions (cm^{-1}) from Laser-Ablated Re Atom Co-deposition with Pure Nitrogen at 10 K

$^{14}N_2$	$^{15}N_2$	R(14/15)	assignment	$^{14}N_2$	$^{15}N_2$	*R*(14/15)	assignment
2226.9	2153.7	1.0340	$(NN)_xNReO$	1083.8	1050.0	1.0322	$(NN)_x{}^{185}ReN$
2204.6	2131.4	1.0343	$Re(NN)_5$	1083.4	1049.6	1.0322	$(NN)_x{}^{187}ReN$
2147.0	2075.6	1.0344	$(NN)_xReN$	1078.3	1044.7	1.0322	$(NN)_xReN$
2136.0	2064.9	1.0344	?	1060.4	1027.2	1.0323	$(NN)_xNReO$
2132.1	2061.2	1.0344	?	887.8	885.4	1.0027	$(NN)_xNReO$
2100.6	2030.8	1.0344	$Re(NN)_x$	862.7	839.2	1.0280	?
2097.7	2028.0	1.0344	$Re(NN)_x$	846.7	821.7	1.0304	?
2087.8	2018.4	1.0344	$Re(NN)_x$	816.5	792.8	1.0299	$Re(NN)_5$
2083.5	2014.2	1.0344	$Re(NN)_5$	522.6	506.5	1.0318	$Re(NN)_x$
2071.5	2002.6	1.0344	$Re(NN)_5$	511.4	494.4	1.0344	$Re(NN)_x$
2003.0	1937.2	1.0340	N_3-	439.7	425.8	1.0326	$Re(NN)_5$
1984.5	1918.7	1.0343	$Re(NN)_x$ site	436.2	422.4	1.0327	$Re(NN)_5$
1982.2	1916.4	1.0343	$Re(NN)_x$				
1944.7	1880.0	1.0344	ReNN ?				
1941.9	1877.3	1.0344	ReNN site				
1894.7	1831.8	1.0343	$Re(N_2)$				
1885.8	1823.3	1.0343	$Re(N_2)$ site				
1744.1	1686.2	1.0343	$Re_2(N_2)$?				
1742.3	1684.4	1.0344	$Re_2(N_2)$ site				
1740.2	1682.3	1.0344	$Re_2(N_2)$ site				
1657.4	1603.3	1.0337	N_3				
1652.5	1598.3	1.0339	N_3 site				
1116.1	1081.1	1.0324	ReN				
1093.7	1059.5	1.0323	$(NN)_xReN$ site				
1089.1	1055.2	1.0321	$(NN)_xReN$ site				

TABLE 6: Infrared Absorptions (cm^{-1}) from Laser-Ablated Re Atom Co-deposition with 2% N_2 in Argon at 10 K

$^{14}N_2$	$^{15}N_2$	*R*(14/15)	assignment
2131.2	2060.3	1.03441	$Re(NN)_x$
2109.4	2039.3	1.03437	$Re(NN)_x$
2083.9	2014.7	1.03435	$Re(NN)_x$
2058.3	1993.0	1.03276	$Re(NN)_x$
2050.0	1981.5	1.03457	$Re(NN)_x$
2033.4	1965.4	1.03460	$Re(NN)_x$
1972.8	1907.7	1.03412	$Re(NN)_2$ site
1966.2	1900.3	1.03468	$Re(NN)_2$
1940.1	1876.3	1.03400	ReNN
1121.4	1086.2	1.03240	ReN blue site
1117.2	1082.3	1.03225	ReN
1115.8	1080.9	1.03229	ReN site
1084.5	1050.5	1.03237	$(NN)_xReN$
1079.1	1045.5	1.03214	$(NN)_xReN$
889.5	886.8	1.00372	?
861.1	857.4	1.00432	?

that 1015 ± 5 cm^{-1} would be a better gas-phase value. The 1001.3 cm^{-1} argon matrix value would then be red-shifted 13−14 cm^{-1}, in line with the matrix shifts for NbO and MoN.

TaN. The bands at 1063.0, 1058.8, 1057.3, and 1055.7 cm^{-1} in the argon matrix decreased after annealing and became one band at 1058.8 cm^{-1} after 40 K annealing. These bands gave nitrogen-15 counterparts at 1029.8, 1025.9, 1024.5, and 1022.8 cm^{-1} and isotopic ratios of 1.0322,1.0321,1.0320, and 1.0321, which are very close to the harmonic diatomic ratio of 1.0324. No counterpart was observed in the mixed isotopic experiments, and accordingly, these bands are assigned to TaN molecules at different matrix sites. A series of weak bands around 973.2 cm^{-1} in the argon matrix, which appeared on annealing at the expense of TaN absorptions, and bands between 962.9 and 979.5 cm^{-1} in the nitrogen matrix all exhibited diatomic isotopic ratios and a single N atom involvement. Although the latter frequencies are about 90 cm^{-1} lower, these bands are suitable for assignment to $(NN)_xTaN$ complexes following the previous work.[10] The present observation of TaN is in good agreement with the 1060 cm^{-1} value reported by Bates and Gruen.[6]

It is suprising that NN complexing made the TaN frequency red-shift about 90 cm^{-1}, which is completely out of line with the approximately 30 cm^{-1} shifts found for YN, WN, NbN, and VN.[10,22,23] Unlike the other two metal nitrides of this group, VN and NbN, which have triplet ground states, the DFT calculation predicted the ground state of TaN to be a singlet, with 1102.7 cm^{-1} fundamental (scale factor 0.96), as also suggested by previous electronic spectra.[6] However, the calculated NNTaN molecule has a triplet ground state, and the singlet is about 24 kcal/mol higher in energy. The calculated Ta−N stretching vibrational frequency of triplet NNTaN (1017.9 cm^{-1}) is just about 85 cm^{-1} lower than the calculated singlet TaN fundamental. Hence, we conclude that the ground electronic state of TaN is changed by the field of complexing N_2 ligands as has been observed for the MnN molecule.[10] Accordingly, the 1058.8 cm^{-1} fundamental observed here for TaN in solid argon points to a 1070 cm^{-1} prediction for the gas-phase vibrational fundamental of TaN.

Experiments with Nb, Ta, and NO in this laboratory[24] have produced the sharp 1001.3 and 1058.8 cm^{-1} bands assigned above to isolated NbN and TaN, respectively, without the corresponding $(NN)_xMN$ complexes. The absence of N_2 in the NO experiments provides further evidence to support the present identification of matrix-isolated NbN and TaN.

ReN. The bands at 1121.4, 1117.2, and 1115.8 cm^{-1} in the argon matrix containing Re + N_2 decreased on higher temperature annealing and produced lower frequency bands at 1084.5 and 1079.1 cm^{-1}. All of these bands showed 14/15 nitrogen isotopic ratios near 1.0322, which is very close to the harmonic diatomic ReN ratio (1.0325). Furthermore, no intermediate component was observed in the mixed nitrogen isotopic experiment, suggesting the motion of a single N atom. In the pure nitrogen matrix, strong bands observed at 1084.9, 1083.6 cm^{-1} after deposition and weak bands at 1116.1, 1089.3, 1086.7 cm^{-1} appeared on annealing and exhibited the same isotopic ratios (1.0322). In the high-resolution spectrum, the main 1083.6 cm^{-1} band split into two bands with a 0.39 cm^{-1} separation, which is near the calculated 0.41 and observed 0.40 cm^{-1} diatomic $^{185}ReN/^{187}ReN$ isotopic splitting.[7] The relative intensities are appropriate for natural abundance ^{185}Re and ^{187}Re and confirm that only one Re atom is involved in the vibration.

TABLE 7: Relative Energies, Geometries, Vibrational Frequencies, and Intensities Calculated (BP86 Functional, D95* Basis Sets for N and LanL2DZ for Metal Atoms) for MN Molecules and NNMN Complexes

molecule	state	relative energy (kcal/mol)	geometry (Å, deg)	frequency, cm^{-1}, (intensity, km/mol)
NbN	triplet	0	Nb−N: 1.694	1034.9 (44)
	singlet	+17.4	Nb−N:1.690	1048.0 (41)
TaN	singlet	0	Ta−N:1.690	1102.7 (56)
	triplet	+2.8	Ta−N:1.702	1041.5 (36)
ReN	triplet	0	Re−N:1.647	1173.5 (38)
	quintet	+28.9	Re−N:1.690	1033.2 (52)
NNNbN	triplet	0	Nb−N:1.701, 2.104	2057.6 (548)
			N−N: 1.147	1029.4 (62)
			∠NNbN:97.6	
	singlet	+7.9	Nb−N:1.697, 2.036	1992.6 (485)
			N−N:1.161	1038.5 (49)
			∠NNbN:98.9	
NNTaN	triplet	0	TaN:1.714, 2.041	2005.5 (450)
			N−N:1.154	1017.9 (39)
			∠NTaN:95.6	
	singlet	+23.3	Ta−N:1.716, 1.980	1953.0 (455),
			N−N:1.168	995.0 (23)
			∠NTaN:97.7	
NNReN	triplet	0	ReN:1.662, 1.943	1988.9 (533)
			N−N:1.159	1118.0 (38)
			∠NReN:109.6	
	singlet	+1.5	Re−N:1.649, 1.891	2046.7 (355)
			N−N:1.155	1158.9 (28)
			∠NReN:97.1	

TABLE 8: Relative Energies (kcal/mol), Geometries (Å, deg) Vibrational Frequencies (cm^{-1}), and Intensities (km/mol) Calculated (BP86 Functional, D95* Basis Sets for N and LanL2DZ for Metal Atoms) for MN_2 Isomers

molecule	state	relative energy	geometry	ν_1(I)	ν_2(I)	ν_3(I)
NbNN	sextet	0	Nb−N:2.017	1916.0(520)	423.5(11)	274.1(5)
			N−N:1.163			
NNbN	doublet	+3.4	NbN:1.754	963.2(19)	313.3(5)	749.8(26)
			∠NNbN = 99.4°			
NNbN	$^4B_2$	+43.0	NbN:1.777	923.5(78)	274.2(0.1)	644.0(0.6)
			∠NNbN = 99.4°			
Nb(N_2)	doublet	+5.6	Nb−N:1.828	1042.5(52)	459.2(1)	740.0(13)
			N−N:1.444			
Nb(N_2)	quartet	+15.0	Nb−N:2.063	1581.7(184)	434.6(0.3)	410.3(1)
			N−N:1.234			
Ta(N_2)	doublet	0	Ta−N:1.796	974.1(29)	343.6(0)	813.9(6)
			N−N:1.567			
Ta(N_2)	quartet	+48.9	Ta−N:2.030	1506.3(203)	411.8(0.3)	296.4(13)
			N−N:1.244			
Ta(N_2)	sextet	+27.7	Ta−N:2.186	1779.7(276)	342.8(1)	177.4(4)
			N−N:1.193			
NTaN	doublet	+8.2	TaN:1.766	945.0(2)	303.2(2)	749.5(12)
			∠NTaN = 98.9°			
NTaN	$^4B_2$	+34.4	TaN:1.771	943.1(43)	263.4(2)	722.3(4)
			∠NTaN = 101.3°			
NTaN(NN)	doublet		Ta−N: 1.173	2186.2(403)	930.1(1)	751.9(8)
			TaN:2.375			
			N≡N:1.132			
			∠NTaN = 103.2°			
NReN	doublet	0	ReN:1.700	1070.6(4)	449.3(0.02)	933.9(188)
			∠NReN = 104.5°			
NReN	quartet	+16.4	ReN:1.722	1026.2(23)	309.7(2)	738.4(13)
			∠NReN = 106.6°			
ReNN	$^4A''$	+13.0	Re−N:1.830	1949.9(381)	582.0(8)	334.9(4)
			NN:1.173			
			∠ReNN:179.4°			
Re(N_2)	$^4B_1$	+25.8	Re−N:1.897	1348.6(61)	539.5(0.1)	593.1(15)
			N−N:1.291			
Re(N_2)	doublet	+38.9	Re−N:1.906	1382.4(80)	517.7(0.3)	582.0(17)
			N−N:1.280			

The 1121.4, 1117.2, 1115.8 cm^{-1} bands in solid argon are very close to the ReN gas-phase fundamental,[7] and it is difficult to know which matrix band is due to isolated ReN and if any of these involve NN ligands. Similar experiments in this laboratory with Re and NO gave the sharp weak 1117.2 cm^{-1} band.[24] Since only trace N_2 can be present, the 1117.2 cm^{-1} band is the favorite for isolated ReN. Clearly, the 1084.5 and 1079.1 cm^{-1} argon matrix bands produced on annealing near the 1083.6 cm^{-1} nitrogen matrix band are due to ligated $(NN)_xReN$. The 1117.2 cm^{-1} argon matrix band is assigned to isolated ReN in the argon matrix, and the 1121.4 and 1115.8 cm^{-1} bands are assigned to matrix sites. The 1116.1 cm^{-1} nitrogen matrix band may also be due to the isolated ReN molecule. This assignment is in very good agreement with the recently reported[7] gas-phase

fundamentals at 1121.9 and 1121.5 cm^{-1} for isotopic ^{185}ReN and ^{187}ReN. The small 4.5 cm^{-1} red-shift by the argon matrix is reasonable. Unlike MnN, which has a quintet ground state, DFT calculations gave a triplet ground state for the ReN molecule with bond length of 1.647 Å, which is in excellent agreement with gas-phase experimental 1.638 Å value.[7] The 1173.5 cm^{-1} calculated frequency is also slightly higher than the experimental observation, as expected for density functional theory (scale factor 0.95).[10,25]

Dinitrides. *NbN_2.* The doublet at 889.6, 888.4 cm^{-1} tracked with the doublet at 651.0, 649.0 cm^{-1} in solid nitrogen, and both produced almost symmetrical 1/2/1 triplets with intermediate bands at 876.9, 875.6 cm^{-1} and 641.1, 639.2 cm^{-1}, respectively. The 1/2/1 triplets indicate that two equivalent nitrogen atoms are involved in the vibration. The 14/15 isotopic ratios for the lower doublet are 1.0299, 1.0295, which are slightly lower than the diatomic NbN ratio (1.0302) and indicate less nitrogen participation than in NbN. These bands are appropriate for the antisymmetric vibration of a bent NNbN dinitride molecule (called NbN_2 for convenience) at different sites. The isotopic ratios for the upper doublet, 1.0307 and 1.0309, are slightly higher than the diatomic NbN ratio and are appropriate for the symmetric vibration of NNbN. This is analogous to the CrN_2 molecule.[10] For terminal position isotopic substitution in a C_{2v} molecule, the 14/15 isotopic ratio predicts a 102 ± 4° upper limit for the NNbN valence angle, owing to differences in anharmonicity between isotopes.[26]

DFT calculations predict the ground state for NNbN as a doublet with a 99.4° valence angle. The ratios of calculated isotopic frequencies, 1.0295 for antisymmetric and 1.0307 for symmetric vibrations, are almost the same as the observed values, but the calculated 963.2 and 749.8 cm^{-1} symmetric and antisymmetric frequencies are slightly higher as expected (scale factors 0.92, 0.87).[10,25] In the N−N stretching region, two weak bands at 2323.0, 2320.4 cm^{-1} have the same annealing behavior and the diatomic nitrogen isotopic ratio (1.0345), and the latter bands are appropriate for an NN ligand. Accordingly, these bands are assigned to vibrations of the NbN_2 molecule in solid nitrogen, i.e., the complexed $(NN)_xNbN_2$ molecule.

The NNbN absorptions increased on annealing in the nitrogen matrix, particularly the mixed isotopic molecule, and showed that this molecule is made from the N + NbN reaction in eq 4.

$$N + (NN)_xNbN \rightarrow (NN)_xNbN_2 \qquad (4)$$

In the solid argon matrix, doublets at 918.6, 914.9 cm^{-1} and 685.4, 680.8 cm^{-1} were observed after deposition and increased on broadband photolysis. In the $^{15}N_2$/Ar experiment, these bands shifted to 891.5, 887.8 cm^{-1} and 665.9, 661.3 cm^{-1} and gave the isotopic ratios 1.0304, 1.0305 for the upper and 1.0293,1.0295 for the lower bands. These bands are suitable for assignment to the isolated NNbN molecule. However, weaker intermediate components were observed at 905.6 and 671.5 cm^{-1} for these bands in the mixed isotopic experiment. This suggests that some NNbN was made by direct insertion of laser-ablated Nb atoms into dinitrogen, reaction 5, whereas some was prepared by the N + NbN reaction; hence, the pure isotopic absorptions were much stronger than the mixed component. Photolysis is also capable of initiating reaction 5.

$$Nb^* + N_2 \rightarrow [NNbN]^* \xrightarrow{\text{relax}} NNbN \qquad (5)$$

TaN_2. Similar behavior was found in the tantalum system. Sharp bands at 895.2, 693.3, and 2296.9 cm^{-1} appeared on annealing in the solid nitrogen matrix. The former two bands exhibited 1/2/1 triplets with mixed isotopic nitrogen sample, indicating that two equivalent nitrogen atoms are involved. The 14/15 ratio for the 693.3 cm^{-1} band (1.0320) and for the 895.2 cm^{-1} band (1.0327) are slightly lower and higher than the harmonic diatomic TaN ratio (1.0324), respectively. These bands are suitable for antisymmetric and symmetric vibrations for a bent NTaN molecule. The 2296.9 cm^{-1} band shifted to 2220.3 cm^{-1} and exhibited the 1.0345 isotopic ratio for N−N stretching vibration. Hence, we assign these bands to the complexed $(NN)_xTaN_2$ molecule. The 922.7 and 740.3 cm^{-1} counterparts in solid argon are probably due to the isolated TaN_2 dinitride molecule.

The DFT calculation gave 945.0 and 749.5 cm^{-1} frequencies for symmetric and antisymmetric vibrations of the ground doublet state NTaN molecule (scale factors 0.95, 0.92). The calculated valence angle 98.9° is in good agreement with the 101 ± 4° upper limit obtained from the observed 14/15 isotopic ratio.[26]

Dinitrogen Complexes. The bands at 2071.7 cm^{-1} and satellite at 2061.6 cm^{-1} together with the bands at 523.0 and 519.0 cm^{-1} were the dominant features in both regions after deposition in the Nb + N_2 system. The large 14/15 isotopic ratio (1.0302) suggests that the 523.0 cm^{-1} band is due to an Nb−NN stretching vibration. This band exhibited a resolved pentet with three strong intermediate components in the $^{14}N_2$ + $^{15}N_2$ experiment, providing evidence for a mode involving four equivalent N_2 subunits. The 14/15 isotopic ratio (1.0343) for the 2071.7 cm^{-1} band is appropriate for N−N stretching mode, but no strong intermediate components were observed in the mixed isotopic experiment, which is characteristic of a degenerate mode.[27] These two bands are assigned to stretching vibrations of the $Nb(NN)_4$ complex.

The sharp band at 2134.8 cm^{-1} went together with the 439.4 cm^{-1} band, as they both grew markedly on annealing. The isotopic ratio 1.0344 for the upper band is appropriate for an N−N stretching vibration, while the 439.4 cm^{-1} band showed the Nb−NN stretching vibration ratio (1.0300). The mixed isotopic structure for both bands was not clear because of band overlap and isotopic dilution, but it is clear that the upper band exhibited an isotopic doublet with no strong mixed isotopic components. Compared to the previous V + N_2 system[10] where similar bands at 2137.7, 455.6 cm^{-1} were assigned to the $V(NN)_6$ molecule, the similar 2134.8, 439.4 cm^{-1} bands are probably due to the analogous $Nb(NN)_6$ molecule.

The weak band at 1965.2 cm^{-1} observed after deposition decreased on annealing, showed a pure N−N nitrogen isotopic ratio and doublet with $^{14}N_2$ + $^{15}N_2$, and is assigned tentatively to the NbNN molecule. The NbNN molecule was calculated to be the most stable isomer at this level of theory and gave a 1916.0 cm^{-1} N−N stretching vibration frequency. Several bands at 2121.3, 2087.8 cm^{-1} and their associated bands at 458.6, 475.1 cm^{-1} cannot be identified and are tentatively assigned to $Nb(NN)_x$ with $2 \le x \le 5$.

Very similar to the Nb + N_2 system, laser-ablated Ta atoms in solid nitrogen produced two strong bands at 2040.9 and 2102.8 cm^{-1}, and, in the low region, two bands at 453.5 and 457.8 cm^{-1} have the same behavior. In the mixed $^{14}N_2$ + $^{15}N_2$ experiment, the 2040.9 cm^{-1} band revealed a strong doublet with three weak intermediate mixed isotopic components between pure isotopic counterparts, and three extra weak bands at higher frequency. This pattern indicates that the 2040.9 cm^{-1} band is due to the triply degenerate mode of $Ta(NN)_4$ with the tetrahedral geometry.[27] The weak upper bands are mixed isotopic counterparts of the corresponding symmetric mode

whose pure isotopic bands are IR inactive. The 453.5 cm^{-1} band had a large (1.0307) isotopic 14/15 ratio and is due to the corresponding Ta−NN stretching vibration of $Ta(NN)_4$. The 2102.8 cm^{-1} band increased markedly on annealing, and the mixed sample exhibited a strong doublet with no obvious intermediate components. The 2102.8 cm^{-1} band and associated 457.8 cm^{-1} band are assigned to $Ta(NN)_6$ following the analogous $Nb(NN)_6$ and $V(NN)_6$ molecules. Finally, a weak band observed at 1947.6 cm^{-1} after deposition decreased on annealing, and only pure isotopic counterparts were observed in the mixed isotopic sample; this band is tentatively assigned to the TaNN molecule.

Laser-ablated Re atoms in solid nitrogen gave rise to strong sharp bands at 2083.5, 2071.5 cm^{-1} and 439.7, 436.2 cm^{-1} after annealing. Weaker 2204.6 and 816.5 cm^{-1} bands increased with the former absorptions on annealing. The stable rhenium carbonyl is the $Re_2(CO)_{10}$ molecule,[28] so the completely ligated $Re_2(NN)_{10}$ molecule and the $Re(NN)_5$ monomer must be considered. The analogous Mn/N_2 study[10] produced evidence for $Mn(NN)_5$ and $Mn_2(NN)_{10}$. The strong, sharp 2083.5 and 2071.5 cm^{-1} bands produced mixed isotopic bands, but it is difficult to make specific assignments. The best course of action is to model with the spectrum of Mn and to follow the C_{4v} $Mn(CO)_5$ molecule, which has weak 2060 cm^{-1} apical and strong equatorial 1938 and 1911 cm^{-1} C−O stretching modes.[29] The 2204.6, 2083.5, and 2071.5 cm^{-1} bands are tentatively assigned accordingly to $Re(NN)_5$, which is presumably a C_{4v} molecule. The 816.5 and 439.7 cm^{-1} bands are due to Re−N−N deformation and Re−NN stretching modes, respectively, for $Re(NN)_5$. Several major bands at 2100.6, 2097.7, 2087.8 cm^{-1} decreased on annealing and are probably due to partly ligated species $Re(NN)_x$ with $x = 3, 4, 5$.

With Re and 2% N_2 in argon, the 1940.1 and 1966.2 cm^{-1} bands appeared on first annealing to 25 K. Using the $^{14}N_2 + {}^{15}N_2$ sample, the 1940.1 cm^{-1} band exhibited a doublet, while the 1966.2 cm^{-1} band gave a triplet, which suggested assignments to ReNN and $Re(NN)_2$.

All three metals in pure dinitrogen matrix gave weak bands around 1800 cm^{-1}. In the Nb/N_2 system, a 1815.6 cm^{-1} band decreased on annealing and gave way to a broad band centered at 1857.1 cm^{-1}. In the Ta/N_2 system, a 1762.6 cm^{-1} band was observed after deposition and decreased on annealing in favor of a broad band centered at 1810.7 cm^{-1}. In the Re/N_2 system, weak bands at 1831.8, 1823.3 cm^{-1} gave way to bands at 1686.2, 1684.4, and 1682.3 cm^{-1} on annealing. These bands red-shifted more than 500 cm^{-1} from the N_2 fundamental and showed pure N−N isotopic ratios. Similar bands observed in the V, Cr, and Mn $+N_2$ system were assigned to cyclic $M(N_2)$ species.[10] However, calculations do not appear to support assignment of these bands to $M(N_2)$. The most stable states for $Nb(N_2)$ and $Ta(N_2)$ molecule were calculated to be doublet with N−N stretching frequencies around 1000 cm^{-1}. Note that the N−N bond length was very large compared with the diatomic nitrogen bond length. So forming these molecules may require a large energy barrier. However, the calculated sextet states were slightly higher in energy and exhibited N−N stretching vibrations around 1800 cm^{-1}, which are in agreement with the present observations. Clearly, the present DFT calculations must be considered only as a first approximation, and higher levels of theory are required for a better description of these novel molecules. Another possibility is that the electronic ground states might be changed by ligand field effects as has been observed for the TaN and MnN molecules and that the $M(N_2)$ submolecules are in the sextet state in the $(NN)_xM(N_2)$ complexes.

Other Absorptions. A sharp 769.8 cm^{-1} band appeared on annealing with Nb. The isotopic ratio 1.0291 was slightly lower than the diatomic ratio, and no intermediate component was observed. This band can be tentatively assigned to the Nb_2N metal cluster nitride molecule. The 724.9, 569.6 cm^{-1} bands appeared together on annealing, and both exhibit higher isotopic ratios than the diatomic NbN ratio; these two bands are tentatively assigned to a nonplanar cyclic Nb_2N_2 molecule.

The band at 770.2 cm^{-1} and its site bands at 773.2, 767.6 cm^{-1} observed on annealing with Ta exhibit a large isotopic ratio (1.0331) and an isotopic triplet of doublets. These bands are due to a higher dinitrogen complex. In the argon matrix, several bands at 813.1, 799.7, 770.7, and 754.7 cm^{-1} also cannot be identified. The 813.1 cm^{-1} band showed a large isotopic ratio (1.0330) and no intermediate component, and it may be due to a metal cluster species.

The bands at 2226.9, 1060.4, and 887.8 cm^{-1} track together on annealing with Re in solid nitrogen, and they are near bands assigned to NReO or (NN)NReO complexes at 2122.8, 1054.7, and 880.2 cm^{-1} in solid argon.[24] Hence, the former bands are probably due to ligated NReO in these experiments arising from a trace of oxide contamination.

Conclusions

Laser-ablated niobium, tantalum, and rhenium atoms have been reacted with nitrogen atoms and molecules during condensation in excess argon and in pure nitrogen gas. The metal nitride molecules NbN, TaN, ReN, and their dinitrogen complexes were trapped and identified by nitrogen isotopic shifts and DFT frequency calculations. The NbN_2 and TaN_2 dinitride molecules were produced on annealing in solid nitrogen and on deposition and increased on photolysis in solid argon. It is interesting to note that the simple DFT/BP86/D95*/LanL2DZ calculations predicted frequencies for NbN, NbN_2, TaN, and TaN_2 with scale factors 0.97, 0.92 and 0.87, 0.96, and 0.95 and 0.92, respectively. Metal dinitrogen complexes were also observed in the higher frequency region and illustrate the affinity of naked Nb, Ta, and Re atoms for the dinitrogen molecule.

Acknowledgment. We gratefully acknowledge N.S.F. support under Grant CHE 97-00116.

References and Notes

(1) Greenwood, N. N.; Earnshaw, A. *Chemistry of the Elements*; Pergamon: Oxford, 1984.

(2) Tsai, M. H.; Sun, S. C.; Tsai, C. E. *J. Appl. Phys.* **1996**, *79*, 6932. Wang, Z.; Kawakami, A.; Uzawa, Y. *J. Appl. Phys.* **1996**, *79*, 7837.

(3) Green, D. W.; Korfmacher, W.; Gruen, D. M. *J. Chem. Phys.* **1973**, *58*, 404. See also: Dunn, T. M.; Rao, M. K. *Nature (London)* **1969**, *222*, 266.

(4) Fletcher, D. A.; Dai, D.; Steimle, T. C.; Balasubramanian, K. *J. Chem. Phys.* **1993**, *99*, 9324.

(5) (a) Féménias, J. L.; Athénour, C.; Dunn, T. M. *J. Chem. Phys.* **1975**, *63*, 2861. (b) Pazyuk, E. A.; Moskvitina, E. N.; Kuzyakov, Yu. Ya. *Spectrosc. Lett.* **1986**, *19*, 627. (c) Féménias, J. L.; Athénour, C.; Rao, K. M.; Dunn, T. M. *J. Mol. Spectrosc.* **1988**, *131*, 113. (d) Azuma, Y.; Barry, J. A.; Lyne, M. P. J.; Merer, A. J.; Schroder, J. O.; Féménias, J. L. *J. Chem. Phys.* **1989**, *91*, 1.

(6) Bates, J. K.; Gruen, D. M. *J. Chem. Phys.* **1979**, *70*, 4428.

(7) Ram, R. S.; Bernath, P. F.; Balfour, W. J.; Cao, J.; Qian, C. X. W.; Rixon, S. J. *J. Mol. Spectrosc.* **1994**, *168*, 350.

(8) Kang, H.; Beauchamp, J. L. *J. Phys. Chem.* **1985**, *89*, 3364. See also: Levy, M. R. *J. Phys. Chem.* **1989**, *93*, 5195.

(9) Chertihin, G. V.; Andrews, L.; Neurock, M. *J. Phys. Chem.* **1996**, *100*, 14609.

(10) Andrews, L.; Bare, W. D.; Chertihin, G. C. *J. Phys. Chem. A* **1997**, *101*, 8417.
(11) Andrews, L.; Citra, A.; Chertihin, G. V.; Bare, W. D.; Neurock, M. *J. Phys. Chem. A* **1998**, *102*, 2561.
(12) Zhou, M. F.; Andrews, L. *J. Phys. Chem. A*, in press (Nb, Ta + O_2).
(13) Frisch, M. J.; Trucks, G. W.; Schlegel, H. B.; Gill, P. M. W.; Johnson, B. G.; Robb, M. A.; Cheeseman, J. R.; Keith, T.; Petersson, G. A.; Montgomery, J. A.; Raghavachari, K.; Al-Laham, M. A.; Zakrzewski, V. G.; Ortiz, J. V.; Foresman, J. B.; Cioslowski, J.; Stefanov, B. B.; Nanayakkara, A.; Challacombe, M.; Peng, C. Y.; Ayala, P. Y.; Chen, W.; Wong, M. W.; Andres, J. L.; Replogle, E. S.; Gomperts, R.; Martin, R. L.; Fox, D. J.; Binkley, J. S.; Defrees, D. J.; Baker, J.; Stewart, J. P.; Head-Gordon, M.; Gonzalez, C.; Pople J. A. *Gaussian 94*, Revision B.1; Gaussian, Inc.: Pittsburgh, PA, 1995.
(14) Perdew, J. P., *Phys. Rev. B* **1986**, *33*, 8822. Becke, A. D. *J. Chem. Phys*. **1993**, *98*, 5648.
(15) Dunning, T. H., Jr.; Hay, P. J. In *Modern Theoretical Chemistry*; Schaefer, H. F. III, Ed.; Plenum: New York, 1976.
(16) Hay, P. J.; Wadt, W. R. *J. Chem. Phys.* **1985**, *82*, 299.
(17) Tiam, R.; Facelli, J. C.; Michl, J. *J. Phys. Chem.* **1988**, *92*, 4073.
(18) Hassanzadeh, P.; Andrews, L. *J. Phys. Chem.* **1992**, *96*, 9177.
(19) Oehler, O.; Smith, D. A.; Dressler, K. *J. Chem. Phys.* **1977**, *66*, 2097 and references therein.
(20) Fletcher, D. A.; Jung, K. Y.; Steimle, T. C. *J. Chem. Phys.* **1993**, *99*, 901.
(21) Sze, N. K.-S.; Cheung, A. S.-C. *J. Quant. Spectrosc. Radiat. Transfer* **1994**, *52*, 145.
(22) Souter, P. F.; Bare, W. D.; Andrews, L., to be submitted (MoN, WN).
(23) Chertihin, G. V.; Bare, W. D.; Andrews, L. *J. Chem. Phys. A* **1998**, *102*, 3697.
(24) Zhou, M. F.; Andrews, L., submitted for publication (Nb, Ta, Mn, Re + NO).
(25) Scott, A. P.; Random, L. *J. Phys. Chem.* **1996**, *100*, 16502.
(26) Allavena, M.; Rysnik, R.; White, D.; Calder, V.; Mann, D. E. *J. Chem. Phys.* **1969**, *50*, 3399.
(27) Darling, J. H.; Ogden, J. S. *J. Chem. Soc., Dalton Trans*. **1972**, 2496.
(28) Levenson, R. A.; Gray, H. B.; Ceaser, G. P. *J. Am. Chem. Soc.* **1970**, *92*, 3653.
(29) Huber, H.; Kundig, E. P.; Ozin, G. A.; Poe, A. J. *J. Am. Chem. Soc.* **1975**, *97*, 308.